Ab initio periodic pseudopotential Hartree–Fock calculations of O_2 dissociation on perfect Si(100) surface

Alexis Markovits, Christian Minot [*]

Laboratoire de Chimie Théorique, UPR 9070 CNRS Université P. et M. Curie, Boîte 137, Tour 23-22 p 114, 4 Place Jussieu 75252, Paris Cédex 05, France

Abstract

This paper investigates the cleavage of O_2 adsorbed on clean Si(100) surfaces with ab initio periodic pseudopotential Hartree–Fock calculations. For the adsorption of the O_2 molecular precursors at coverage $\theta = 1$ (one O_2 per dimer), the Si(100) surface remains reconstructed and O_2 are adsorbed on the dimers, parallel to the surface; the sites between the dimers are vacant. For the atomic adsorption at the same coverage (representing then one O per surface Si) the surface reconstruction nearly disappears; the oxygen atoms are adsorbed over the successive spaces between adjacent surface Si atoms along the (110) directions (those of the elongated dimers and those between them) in asymmetric fashion. The dissociation of O_2 requires the breaking of two bonds, the SiSi and OO bonds and the migration of an oxygen atom. It therefore implies the presence of a high activation energy. Two paths are investigated for the O_2 dissociation and the migration of an atomic oxygen on the surface. The migration of O_2 from the best adsorption mode to least favourable one where the dissociation is easier is also discussed.

Keywords: Hartree–Fock periodic calculations; Adsorption; Oxidation; Silicon

1. Introduction

The adsorption of oxygen on Si(100) have been the object of many studies [1] since it is of great interest in semiconductor technology [2–4]. Silicon is indeed the most used semiconductor; one of the reason is associated to the good quality of its oxide [5]. Hence, a knowledge at the scale of the atomic structure of the oxygen adsorption could help to understand the oxidation process of the silicon at the silicon–silica

interface [6] and help to control metal-oxide-semiconductor devices.

The dissociation of O_2 on the surface is exothermic. However, both O and O_2 species can be identified on Si surfaces [1]. Many experimental studies concluded that there is a metastable molecular precursor [7,8] in the initial stage of oxidation of Si surfaces. Its structure is however still unclear [9]. O_2 is physisorbed as a metastable species up to 90 K [1]. Its cleavage on the surface seems to be difficult at room temperature and, according to Ciraci [10], dioxygen might coexist with atomic oxygen on the surface. Several spectroscopy experi-

---

[*] Corresponding author.

ments at low coverage reveal both atomic and molecular chemisorbed species on Si surfaces [1,11]. STM experiments [12] show that majority sites of the dimers appear to be unreactive under O_2 exposures. Thus the dissociation would not occur on perfect surfaces and would only take place on defect sites.

The activation barrier on Si(100) face is experimentally estimated to 60 kcal/mol [13], a large value compared with that on Si(111) (0.9 kcal/mol) [14] or Si(111)7 × 7 (5.5 kcal/mol) [15]. Ab initio cluster calculations (HF with 3-21G basis sets and with MP2 perturbation) for the reaction mechanism in the triplet state (O_2 in the initial state is weakly bound; Si–O = 4.46 Å) lead to 60.4 kcal/mol [9] while LDA calculations did not mention an activation barrier.

In this paper, we shall first present the adsorption of a molecular oxygen and atomic oxygen at saturation ($\theta = 1$, one O_2 per dimer or one O per surface Si). The optimized structures are compared with corresponding clusters. The most stable systems when the adsorption is completed is in the singlet state.

The dissociation process involves a migration of an oxygen atom from one place, in the space between two adjacent silicon atoms, to another, in the following space. We calculate intermediate points on the reaction path for this displacement. The O atom has to rotate over a silicon surface, passing through an atop position. Several paths leading to this intermediate situation are investigated.

2. Method of calculation and surface models

Surface calculations have been made with the ab initio periodic-Hartree–Fock program CRYSTAL [16] with a restricted HF Hamiltonian. This program solves the Hartree–Fock–Roothaan equations. A basic unit cell is periodically repeated in two dimensions to generate a slab. The method is described by Pisani et al. [17]. For the oxygen atom, we have used the PS-31G basis set derived from Bouteiller et al.

Table 1
Silicon basis set. For the bulk, the optimized Si–Si distance is 2.416 Å and the cohesive energy per silicon atom 67 kcal/mol (2.377 Å and 82.2 kcal/mol when polarization functions are added). The atomic energy is less stable than that for the basis set optimized for the atom [18] by 11 kcal/mol

Exponent	s-coefficient	p-coefficient
2.8405	0.12403	0.007945
1.4041	−0.38989	0.007033
0.35	1.0	1.0
0.14	1.0	1.0

[18,19]. For the silicon atom, we have modified the two most diffuse sp shells of the PS-211G basis sets used for the bulk stishovite, SiO_2 [19] to improve the description of the silicon bulk (see Table 1). Polarisation functions are not added in the present study. Such functions do not introduce substantial differences for the optimized geometry and the stabilization energy as found by Hoshino [20] and confirmed by our preliminaries studies. They would improve the cohesive energy of the diamond Si bulk by 15 kcal/mol per Si atom. We have used the Durand and Barthelat effective core pseudopotentials [21].

The adsorption energies have been calculated according to the expression:

$$E_{ads} = E_O + E_{slab} - E_{(O + slab)} \qquad (1)$$

where $E_{(O + slab)}$ is the total energy of the oxidized slab, E_O is the Unrestricted Hartree–Fock energy of an isolated oxygen atom in the triplet state (− 15.631872 a.u. according the calculations of Bouteiller et al. [18]) and E_{slab} is the energy of the optimized reconstructed slab. A positive energy corresponds to a stable adsorbate/substrate system.

As well-known, the ground state for dioxygen is $^3\Sigma_g$, lower in energy by 22.5 kcal/mol than the singlet state $^1\Delta_g$. At the PS-31G* level, the dissociation energy ($O_2(^3\Sigma_g) \rightarrow 2O(^3P)$), is − 37.7 kcal/mol; this is close to the SCF limit. CI is required to approach the experimental value, 120.6 kcal/mol [22]. Without polarization function, the stability of the molecule is
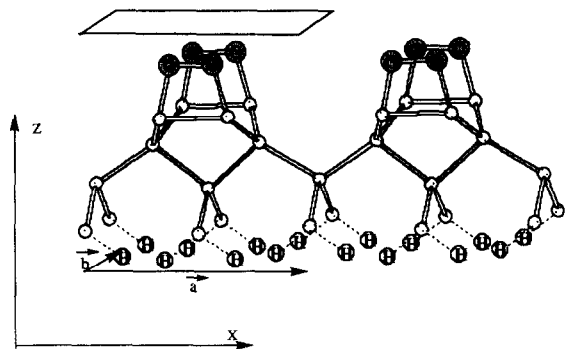
Fig. 1. The model contains four layers of Si atoms (small circles); the dangling bonds of one of the side of the slab are saturated with hydrogen atoms (5th layer) The $p(2 \times 1)$ unit cell is represented by the rectangular above the oxygen atoms. The lengths of the cell vectors are $a = 7.68$ Å and 3.84 Å ($d_{Si-H} = 1.48$ Å). The $p(2 \times 1)$ unit cell contains only one dioxygen molecule, eight silicon atoms (two per layer) and four hydrogen atoms per unit cell. The figure shows the most stable adsorption mode for O_2 (peroxo mode).

strongly reduced whereas the reference energy does not change so that the dissociation energy becomes endothermic $+8.4$ kcal/mol. The barrier to dissociation is however very large.

Our model of the Si(100) surface is a slab consisting of four layers of Si atoms; one of the side of the slab represents the Si(100) surface, the dangling bonds of the opposite side of the slab are saturated with hydrogen atoms (see Fig. 1). The Si–H distance is 1.48 Å.

In the present paper, we have only considered the $p(2 \times 1)$ unit cell. The clean Si(100) surface is reconstructed. Surface atoms form dimers; this induces a reorganization of the sublayers. We have coupled all the motions of the sublayer atoms and define a single parameter for the dimerization degree; a zero parameter corresponds to the unreconstructed surface (SiSi = 3.84 Å) and a parameter of one corresponds to the reconstructed surface given by Roberts [23] (SiSi = 2.19 Å). When the parameter is x, the Si–Si distance of the dimer is $2.19 + x(3.84 - 2.19)$ Å and all the motions of the sublayers are calculated in a similar way.

We have also calculated small cluster models for adsorption using the MONSTERGAUSS program [24]. The same basis sets have been used. The purpose of these calculations is dou-

ble. The geometry of the optimised clusters have been transferred to the CRYSTAL [16] calculations to be used as initial guess before an optimisation on the periodic system. Moreover, the small clusters and their carbon analogues can also be seen as existing molecules (epoxides, ketones, peroxo compounds...) as will been shown more extensively elsewhere. The various adsorption modes can therefore be identified as closed shell systems. The only exception is the perpendicular mode for the adsorption of a dioxygen molecule (triplet state). The dissociation on the surface is exothermic. As it begins and ends by a singlet state, one could expect in a preliminary study that it could be performed by an easy atomic migration on the surface.

3. The best adsorption modes for O_2/Si(100) and O/Si(100)

3.1. O_2/Si(100)

We have performed calculations of the molecular adsorption allowing the dimerization of the surface atom with no buckling at $\theta = 1$ (one O_2 per dimer). This represents the saturation; the distances between adsorbates for an adsorption parallel to the surface (and in the 110 plane) is too short to allow larger coverages.

Under O_2 adsorption, the dimerization remains ($d_{SiSi} = 2.34$ Å) and the adsorption mode 'on the dimer' is the best. This adsorption mode is the bridging peroxo shown in Fig. 2a. The geometry calculated on the periodic crystal is very close to that obtained with $Si_2H_4O_2$ in the singlet state. The SiO distance is slightly larger than the value for SiO_2 (1.77 Å for the periodic calculation, 1.72 Å in the cluster model and 1.61 Å in quartz [25]). The O–O distance, 1.50 Å for the periodic calculation, 1.48 Å for the cluster model, is long compared to that, 1.45 Å, on Si(111) [15,26] and corresponds to a single O–O bond. The SiSi bond length also corresponds to a single bond. The electronic distribution is very similar in the periodic calculation
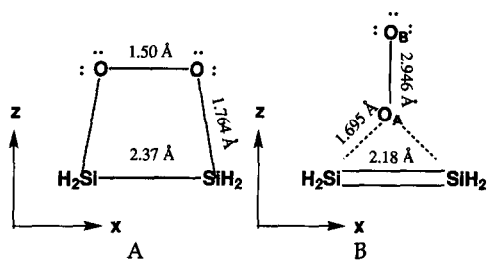
Fig. 2. Cluster models for the molecular adsorption of O_2. (A) H_2Si–O–O–SiH_2 as model for the di-σ or 'bridging peroxo' adsorption. O_2 is assumed to be inserted on the dimers of the reconstructed surface. (B) H_2Si–$O_A(O_B)$–SiH_2 as model for the 'bridging perpendicular' mode. O_2 is assumed to be inserted on the dimers of the reconstructed surface. Distance are those for the triplet state. In the periodic calculations, the adsorption patterns are similar. The distances are OO = 1.50 Å, SiO = 1.77 Å and SiSi = 2.34 Å for case A ('bridging peroxo' adsorption) and OO = 1.66 Å, SiO = 1.76 Å and SiSi = 2.29 Å for case B ('bridging perpendicular' mode).

and in the $Si_2H_4O_2$ model; however for the periodic calculation at saturation, the heat of adsorption, 49.5 kcal/mol, is weaker than that for the cluster model, 57.7 kcal/mol. Note that the use of a larger cluster would reduce the difference: We performed a calculation for the $Si_6H_{12}O_2$ cluster with the Si–Si and Si–O interatomic distances of the system optimized on the periodic model, and we found that the heat of adsorption is 50.4 kcal/mol.

The $Si_2H_4O_2$ structure is reminiscent of a peroxo compound and is very close to that presented by Hoshino et al. [20] or by Zheng [27] who finds binding energies of 82.8 and 49.6 kcal/mol, respectively.

In our periodic calculations, O_2 is more stable parallel to the surface than perpendicular (Fig. 2b) by 46.9 kcal/mol. The conversion from the parallel mode to the perpendicular mode however goes through a barrier of 94.2 kcal/mol. We show the energy profile in Fig. 3, where the rotation of the O_2 molecule is coupled with a shift of its center of mass in order to keep the Si–O_A distance equal to 1.77 Å. We have reoptimized the least stable point from Fig. 3 ($x = 0.48$) by removing the constraints on the OO distance and found no change (the interpolated value, 1.59 Å, is the best one); thus the

activation barrier seems to be reliable. In Section 4.4 we will present another path for this conversion.

In the cluster $Si_2H_4O_2$ model, the lowest state for the perpendicular adsorption mode is a triplet state (more stable than the singlet by 32.2 kcal/mol) with a very long O–O distance (2.95 Å). This state corresponds to the final products obtained by Hoshino [9].

3.2. O / Si(100)

At saturation, the most favourable adsorption mode for the atomic oxygen is a bridging mode the reconstruction is much less pronounced than those for the clean surface or for the molecular adsorption but an asymmetry remains; the O atoms are bridging each SiSi space in the (110) direction, but not symmetrically. The adsorption energy (per O atom at $\theta = 1$) is 55.5 kcal/mol in the periodic calculation (111 kcal/mol per two O to be compared with the corresponding value for O_2 adsorption); this is less than in the corresponding cluster calculation, 81.8 kcal/mol. The heat of adsorption for the peri-
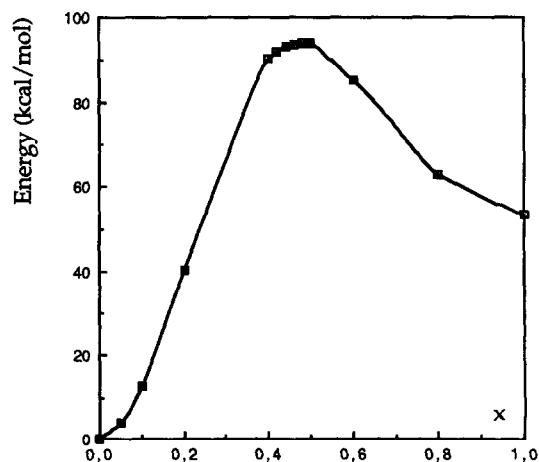

Fig. 3. Energy profile for conversion of the bridging O_2 from the parallel peroxo mode to the perpendicular mode. When x varies from 0 to 1, the angle θ of OO with the x axis varies from 0° to 90°; h, the distance from the O_2 mass center to the surface varies from 1.713 Å to 2.167 Å; d_{OO} from 1.5 Å to 1.68 Å and d_{SiSi} from 2.34 Å to 2.29 Å. The TS takes place at $x = 0.48$ ($\theta = 43°0.2$; $h = 1.811$ Å; $d_{OO} = 1.59$ Å).
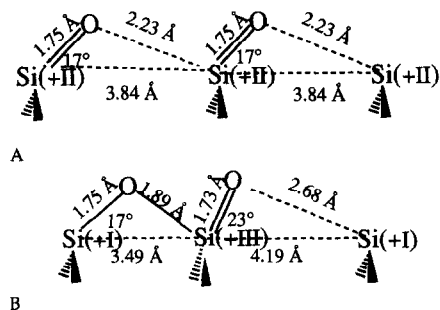
Fig. 4. Atomic adsorption at $\theta = 1$. (a) On the unreconstructed (100) surface; all the O atoms are equivalent. (b) Allowing reconstruction; this pattern distinguishes two kinds of adsorbed oxygen. The decrease of the SiSi distance does not generate dimers but differentiates the surface silicon atoms.

odic calculation at $\theta = 1/2$ is 54.2 kcal/mol. The oxygen adsorption to increase the coverage from $\theta = 1/2$ to $\theta = 1$ is larger, 56.7 kcal/mol. The comparison between these two values seems to indicate that the saturation is easy to obtain.

The decrease of the magnitude of the dimerization is natural; indeed, for the unreconstructed surface, the presence of 2 DB's on each surface atom suggests the insertion of bridging oxygen atoms in every SiSi space. This allows the saturation of all the dangling bonds. This leads to the structure shown in Fig. 4a where all the surface Si have the same oxidation number, II. However, the SiSi space is too large to allow a symmetric bridging and the oxygen atom stands close to one silicon and far from the other. The total energy is slightly improved when two silicon atoms are moved in a dimerization process. Despite a rather small energy gain, 3 kcal/mol, this motion generates significantly different SiSi spaces (3.49 Å and 4.19 Å) but not really builds a SiSi bond; the smallest value remains large as compared to a SiSi single bond distance (~ 2.35 Å). The bridging O atom on the short space makes two bonds (1.75 Å and 1.89 Å) with the silicon atoms whereas the other one is bound to only one silicon (see Fig. 4b). Thus, this adsorption mode involves two oxidation states for the surface silicon atoms, $Si(+I)$ and $Si(+III)$. The amplitude of this reconstruction is too weak to qualify the reconstructed surface as dimerized.

The *atop adsorption* of the atomic oxygen, corresponds to the $H_2Si=O$ model that is isolobal to the formaldehyde. For the molecular model, its formation from O and H_2Si (singlet as ground state) is exothermic by 45.1 kcal/mol. The SiO distance, 1.55 Å, is short as expected from a double bond. A comparable distance, 1.52 Å, is found in SiO_2 tridymite [25]). The optimized structure is slightly distorted from the planarity (The angle of SiO axis with the planar is 5°). In the periodic calculation, the geometry is very similar (SiO = 1.55 Å). At $\theta = 1$, the adsorption energy is smaller than in the molecular calculation, 25.7 (26.4 kcal/mol for a very slight reconstruction). The dissociation leading to this mode $O_2(ads) \rightarrow 2O(atop)$ is nearly athermic ($-1.9 / -3.3$ kcal/mol).

4. The dissociation

4.1. Passing through the atop adsorption, general scheme

From the results of the previous section, the dissociation $O_2(ads) \rightarrow 2O(ads)$ is exothermic by 61.4 kcal/mol.

Going from O_2 adsorbed in the peroxo mode to 2O adsorbed in bridged positions requires the cleavage of two bonds, O–O and Si–Si and the migration of one oxygen atom from the space on the dimer to that within the dimers. During this process, the migrating oxygen has therefore to pass through an atop position. Fig. 5 sketches this situation and distinguishes a symmetric path A and an asymmetric path B. Path A leads in a first step A1 to the atop adsorption; this step is nearly athermic whereas the following step, A2, is exothermic. For path B, we show as intermediate the situation with one atop oxygen atom coadsorbed with another O optimized in its best adsorption mode. Then, the oxygen atom bridges the SiSi space with a quasi linear fashion. The first step is also nearly athermic and the second step exothermic. We have investigated the first
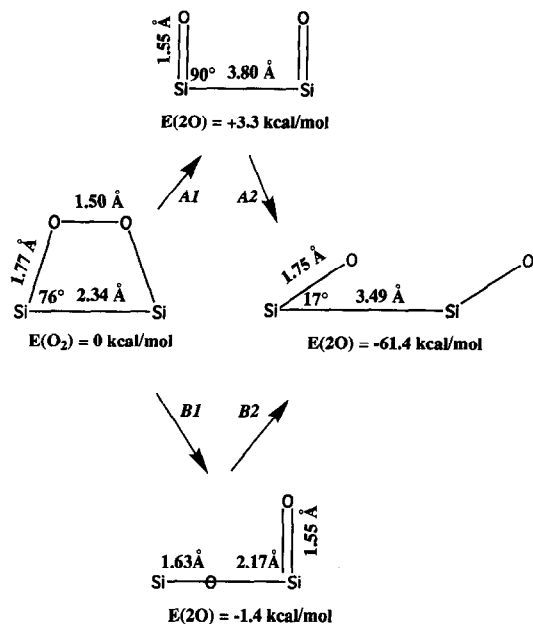
Fig. 5. Symmetric (A) and asymmetric (B) paths for the dissociation of O_2 on the surface. The reference energy is the most stable adsorption of O_2. The rotation of O around Si at 1.63 A for the B intermediate $E(2O)$ is free (1 kcal/mol).

steps, A1 and B1, to search for an activation barrier.

4.2. The symmetric path, step A1

To reduce the large number of parameters, we have made several assumptions and coupled in different ways the variations of the parameters. Fig. 6a represents the energy profile for path A1 assuming a concerted mechanism: all the parameters are assumed to vary in the same ratio. The energy barrier is very large, ∼ 208 kcal/mol. The concerted mechanism is clearly not favourable. It corresponds to the reverse reaction of a 2 + 2 cycloaddition, forbidden by the Woodward–Hoffmann rules. A molecular model (see Fig. 2a), leads to a large barrier (Fig. 6b), but not as important as the periodic calculation. Fig. 7 shows the decomposition of step A1 into two successive cleavages, the O–O cleavage preceding or following the SiSi cleavage. The barrier takes place during the first cleavage made. When the silicon dimer is elongated at

first, the barrier is lower, ∼ 103 kcal/mol than when the dioxygen is cleaved in the first step, ∼ 218 kcal/mol. For a two step mechanisms,
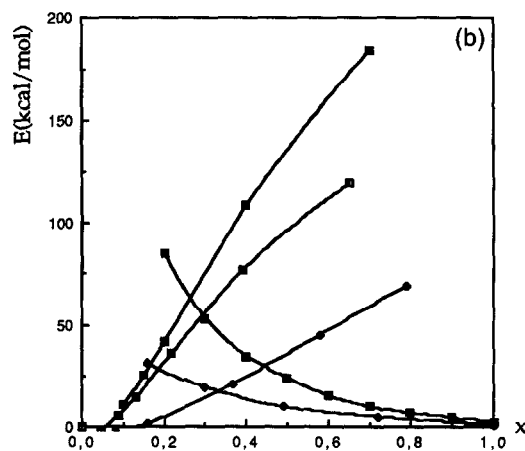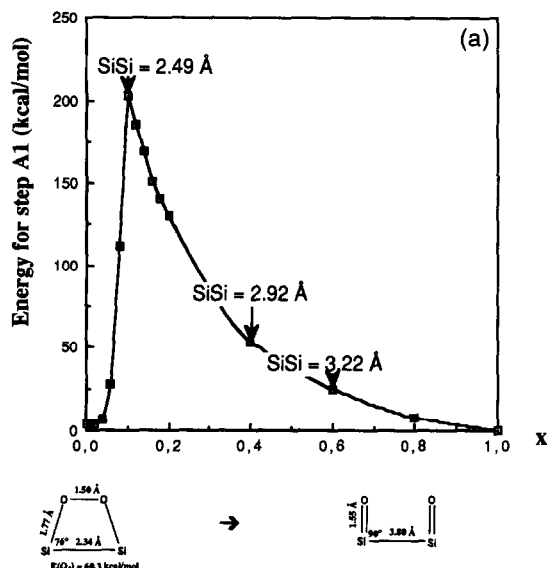

Fig. 6. (a) Energy profile for concerted mechanism for path A1. x is the reaction coordinate (d_{SiSi} = 2.34 → 3.80 Å; d_{OO} = 1.50 → 3.80 Å; d_{SiO} = 1.77 → 1.55 Å). (b) Energy profile for two steps mechanism for path A calculated with the cluster model. The higher curves (starting from both sides) corresponds to the concerted mechanism (SiSi and OO are simultaneously elongated ($x = 0 → 1$) or shortened ($x = 1 → 0$). All the other parameters are optimized. In the region for the 'transition state', we obtain two different states according to the initial state. The lower curves ($x = 0 → 1$) corresponds to the elongation of OO (intermediate curve) or SiSi with an optimization of all the other geometric parameters. The lowest curve ($x = 1 → 0$) corresponds to the shortening of SiSi with an optimization of all the other geometric parameters.
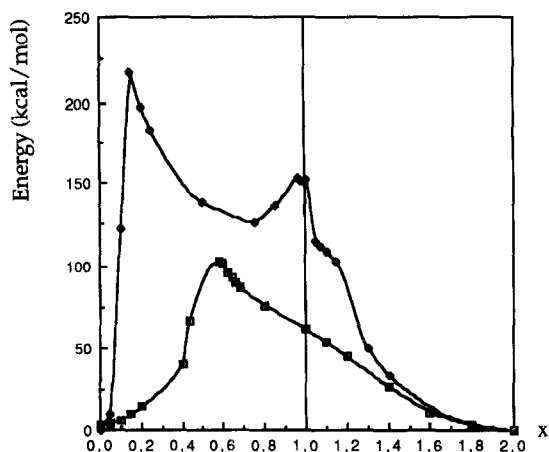
Fig. 7. Energy profile for two steps mechanism for path A1. In the lower curve, at first ($x = 0 \rightarrow 1$), the SiSi distance is elongated from 2.34 Å to 3.8 Å; the OO distance is elongated next ($x = 1 \rightarrow 2$). The TS corresponds to $x = 0.58$ ($d_{SiSi} = 3.19$ Å). The higher curve corresponds to the opposite situation. The second peak (a shoulder at $x = 0.96$) corresponds to a repulsion between the O atoms and the silicon atoms from the first layer below the surface and disappears when some amount of concertation is introduced. In both cases, the shortening of the SiO bond is associated to the OO cleavage.
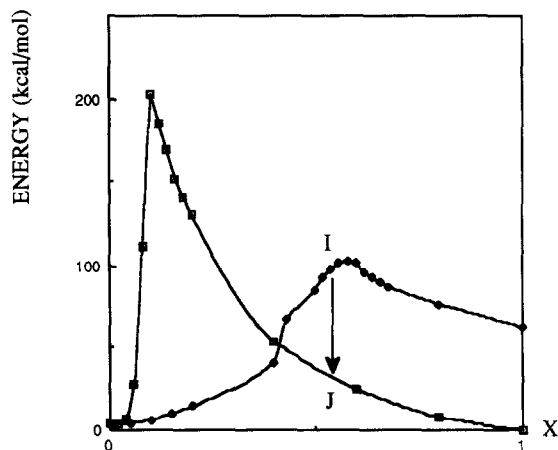

Fig. 8. Energy profile for concerted and two steps mechanisms for path Al as a function of x as defined in the two previous captions. In both cases x represents an elongation of the Si–Si distance. However, for one curve this elongation is accompanied by a simultaneous elongation of the O–O distance, whereas for the other it is not. The 'jump' from one curve to the other requires to increase the O–O distance. The lowest path corresponds to increase the SiSi distance first up to point I, next to cleave the OO bond with no barrier (arrow IJ).

the O–O cleavage follows the SiSi cleavage; the first step corresponds to the disappearance of the surface reconstruction. As for the clean surface where the variation of the dimer bond length corresponds to a flat energy surface, the increase of the SiSi distance is not very destabilizing at the beginning. It becomes however strongly destabilizing under adsorption for SiSi $= 3.19$ Å (a barrier of ~ 103 kcal/mol versus one of ~ 60 kcal/mol for SiSi ~ 2.8 Å for the clean surface).

For the SiSi elongation, the concerted path and the non concerted path (see Fig. 8) cross at $x = 0.4315$ (SiSi $= 2.97$ Å) with an energy of 44.7 kcal/mol. Beyond that point, the OO elongation for a fixed SiSi distance is exothermic and it would be attractive to jump from the upper curve to the lower curve. For $x \sim 0.4$–0.5, the OO overlap population is positive and the OO elongation requires to pass an activation barrier E_1 (see Table 2) corresponding to a very small increase (see coordinate x' in Table 2). For $x = 0.54$ (slightly before the TS for the

two-step mechanism), the OO overlap population becomes zero and OO cleaves without activation barrier. Thus, the lowest path corresponds to an increase of the SiSi bond up to 3.128 Å (point I in Fig. 8) followed by the OO cleavage (arrow IJ in Fig. 8). The activation energy is the value obtained at $x = 0.54$ without allowing OO elongation (Fig. 7), 97.3 kcal/mol.

Table 2
Activation energy, E^*, for the path Ala when the d_{O-O} is optimized; SiSi is elongated (x is the reaction coordinate). E_0 is the energy at fixed d_{O-O} distance, 1.5 Å. E_1 is the activation energy for increasing the d_{O-O} distance from 1.5 Å to the value for the concerted mechanism, see the vertical arrow in Fig. 8 (x' is the corresponding reaction coordinate). For $x < 0.58 E^* = E_0 + E_1$; if the OO elongation takes place beyond $x = 0.58$, the barrier is 102.6 kcal/mol (obtained for the elongation of SiSi)

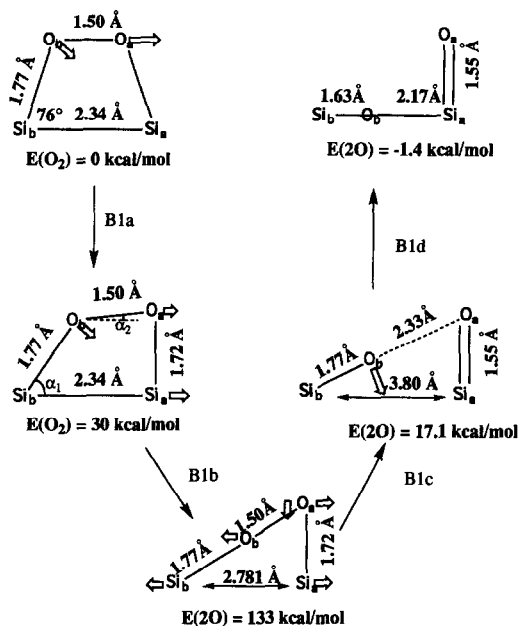| SiSi (x)	OP	E_0	d_{O-O} (x')	E_1	E^*
2.924 (0.4)	0.068	37.4		> 89	> 126.5
2.995 (0.45)	0.058	70.7	1.637 (0.13)	46.6	117.3
3.07 (0.5)	0.036	85.3	1.629 (0.11)	19.9	105.3
3.10 (0.52)	0.023	92.7	1.576 (0.06)	12.1	104.8
3.128 (0.54)	0.000	97.3		none	97.3
3.158 (0.56)	−0.097	102.1		none	102.1
3.187 (0.58)	−0.135	102.6		none	102.6
3.216 (0.60)	−0.162	101.6		none	102.6

Fig. 9. Different paths for an asymmetric cleavage of O_2. The reference energy is the molecular adsorption.

4.3. The asymmetric path, step B1

We have investigated the asymmetric path B (Fig. 5). Step B1 has been decomposed into several successive motions shown in Fig. 9. First, in step B1a, the oxygen O_a is translated to the atop position; the motion is parallel to the surface and decreases the SiO_a distance from 1.77 Å to 1.72 Å. During this motion, the atom O_b moves to remain at 1.77 Å from Si_b and at 1.5 Å from O_a. This step corresponds to a progressive destabilization of 30 kcal/mol with no activation barrier. Next (step B1b), Si_bSi_a is increased up to 2.78 Å and O_b is rotated up to become collinear with Si_bO_a; during this step OO remains at 1.5 Å; the SiSi cleavage has started but not the OO cleavage. In the third step (step B1c), the space between Si_aO_a and Si_bO_b is increased to reach 3.8 Å and the Si_aO_a distance is shortened from 1.72 Å to 1.55 Å. Finally, O_b is rotated up to become collinear with Si_bSi_a (step B1d). These last steps correspond to stabilizations. The step B1b leads to a highly destabilized intermediate, ~ 130 kcal/mol. Thus, the asymmetric path appears less favourable than the symmetric one.

4.4. The conversion from the peroxo O_2 to the perpendicular O_2

A first path has been discussed in Section 3. The shift of O_2 performed in step B1a (Fig. 9) leads to an intermediate that may also lead to the perpendicular adsorption mode of O_2 if the Si_aO_a bond breaks and if an O_bSi_a bond is formed. This represents an alternative path for the O_2 conversion from the peroxo adsorption mode to the perpendicular one. Assuming again a proportionality for the variations of the geometric parameters, we have found an energy barrier of 85.6 kcal/mol ($x = 0.4$, OO = 1.57 Å, $\alpha_1 = 56°2$ and $\alpha_1 = 39°8$, see Fig. 9). This barrier is slightly lower than that proposed in Section 3.1 (see also Fig. 3). Note that this activation barrier remains high, meaning that the transition structure is no longer absorbed.

5. Conclusion

Our calculations show that, in spite of the weak difference in energy between the different adsorption modes, the dioxygen is not mobile on the surface and does not cleave well. The activation barrier for these processes are high and the molecular adsorption can coexist with atomic adsorption as metastable species. We acknowledge that these calculations are limited due to computational constraints (no correlation, limited basis set, RHF Hamiltonian); therefore the barrier might be overestimated. A new version of the CRYSTAL program (CRYSTAL 95) will soon be available allowing us to complete this preliminary work, performing CI and UHF calculations. However, starting from the best adsorption mode for O_2, the peroxo mode, two dissociation paths emerge, having activation barriers above 85 kcal/mol and below 100 kcal/mol. Experimentally, the dissociation energy for the gas phase dissociation ($O_2(^3\Sigma_g^-) \rightarrow 2O(^3P)$), is 120.6 kcal/mol [22]. The symmetric path (labelled A) is a real cleavage on the surface; O_2 appears as a precursor for the atomic adsorption. This path requires an elongation of

the dimers that goes with a weakening of the OO bond; this bond cleaves when the dimer is remarkably elongated and when the O–O Mulliken overlap population vanishes. The alternative way is a migration of the dioxygen from the peroxo mode to the perpendicular mode. This migration requires an activation energy of 85 kcal/mol, but ends with a state whose energy is only 47 kcal/mol above the peroxo. From there, the O_2 dissociation is easy. An elongation by 1 Å of the OO distance costs 17.5 kcal/mol only (leading to 64.5 kcal/mol above the peroxo adsorption mode). This motion leads to the atomic desorption (an atomic adsorption at $\theta = 1/2$ for the O that remains); the O atom expelled in the gas phase is then available for an adsorption on a different site. A conversion to the triplet state would facilitate such cleavage and desorption. This conversion would already require an O_2 desorption–adsorption process populating the least stable adsorption site. Such adsorption–desorption process is fundamentally different from an atomic migration of the adsorbed O species generated from an O_2 precursor. Adsorbed O_2 would generate atomic oxygen involved in a direct adsorption: From the O_2 cleavage the oxygen atom that remains on the surface would be a single whereas that desorbed would be triplet for an eventual direct adsorption.

Difficulties to find a dissociation on perfect surfaces are consistent with the coexistence of molecular and atomic oxygen on the surfaces; it also suggests that dissociation would not occur on perfect surfaces but would take place on defect sites.

Acknowledgements

References

[1] T. Engel, Surf. Sci. Rep. 18 (1993) 91.
[2] P. Balk, Mater. Sci. Monogr. (1988) 32.
[3] R.B. Fair, in: Microelectronics Processing: Chemical Engineering Aspects, American Chemical Society, Washington, DC, 1989.
[4] E.A. Irene, CRC Crit. Rev. Solid State Mater. Sci. (1988) 14.
[5] C.J. Sofield and A.M. Stoneham, Semicond. Sci. Technol. 10 (1995) 215.
[6] F.J. Himpsel, F.R. McFeely, A. Taleb-Ibrahimi, J.A. Yarmoff and G. Hollinger, Phys. Rev. B 38 (1988) 6084.
[7] H. Ibach, H.D. Bruchmann and H. Wagner, Appl. Phys. A 29 (1982) 113.
[8] U. Höfer, P. Morgen, W. Wurth and E. Umbach, Phys. Rev. Lett. 55 (1985) 2979.
[9] T. Hoshino, M. Tsuda, S. Oikawa and I. Ohdomari, Phys. Rev. B 50 (1994) 14999.
[10] S. Ciraci, S. Ellialtioglu and S. Erkoc, Phys. Rev. B 26 (1982) 5716.
[11] C. Silvestre and M. Shayegan, Solid State Commun. 77 (1991) 735.
[12] P. Avouris and I.W. Lyo, Appl. Surf. Sci. 60–61 (1992) 426.
[13] J.R. Engstrom, M.M. Nelson and T. Engel, J. Vac. Sci. Technol. A 7 (1989) 1837.
[14] C. Silvestre and M. Shayegan, Phys. Rev. B 37 (1988) 10432.
[15] U. Höfer, P. Morgen and W. Wurth, Phys. Rev. B 40 (1989) 1130.
[16] R. Dovesi, C. Pisani, C. Roetti, M. Causa and V.R. Saunders, Crystal, Indiana University, IN, 1988.
[17] C. Pisani, R. Dovesi and C. Roetti, in: Hartree–Fock Ab Initio Treatment of Crystalline Systems, Vol. 48, Lecture Notes in Chemistry, Springer, Berlin, Heidelberg, New York, London, Paris, Tokyo, 1988.
[18] Y. Bouteiller, C. Mijoule, M. Nizam, J.C. Barthelat, J.P. Daudey, M. Pelissier and B. Silvi, Mol. Phys. 65 (1988) 295.
[19] B. Silvi, L.-J. Jolly and P. D'Arco, J. Mol. Struct. 260 (1992) 1.
[20] T. Hoshino, M. Tsuda, S. Oikawa and I. Ohdomari, Surf. Sci. Lett. 291 (1993) L763.
[21] P. Durand and J.C. Barthelat, Theor. Chim. Acta 38 (1975) 283.
[22] K.P. Huber and G. Herzberg, in: Molecular Spectra and Molecular Structure, Vol. IV. Constant of diatomic Molecules, Van Nostrand, Princeton, NJ, 1979.
[23] N. Roberts and R.J. Needs, Surf. Sci. 236 (1990) 112.
[24] R.A. Poirier and M. Peterson, Monstergauss (Dept. of Chemistry Memorial University of Newfoundland, St. John's, Nfld, Canada, 1989).
[25] R.W.G. Wyckoff, in: Crystal Structures, Vol. 1, Wiley, New York, 1963.
[26] U. Höfer, A. Puschmann, D. Coulman and E. Umbach, Surf. Sci. 211–212 (1989) 948.
[27] X.M. Zheng and P.V. Smith, Surf. Sci. 232 (1990) 6.